5-2003

Observations on the distribution of meroplankton during an upwelling event

AL Shanks

J Largier

J Brubaker
Virginia Institute of Marine Science

Recommended Citation

Shanks, AL; Largier, J; and Brubaker, J, Observations on the distribution of meroplankton during an upwelling event (2003). *Journal of Plankton Research*, 25(6), 645-667.
10.1093/plankt/25.6.645

JOURNAL OF PLANKTON RESEARCH | VOLUME 25 | NUMBER 6 | PAGES 645–667 | 2003

Observations on the distribution of meroplankton during an upwelling event

ALAN L. SHANKS*, JOHN LARGIER[1] AND JOHN BRUBAKER[2]

OREGON INSTITUTE OF MARINE BIOLOGY, UNIVERSITY OF OREGON, PO BOX 5389, CHARLESTON, OR 97420, [1]SCRIPPS INSTITUTION OF OCEANOGRAPHY, UNIVERSITY OF CALIFORNIA, SAN DIEGO, CA 92093-0209 AND [2]VIRGINIA INSTITUTE OF MARINE SCIENCE, SCHOOL OF MARINE SCIENCE, COLLEGE OF WILLIAM AND MARY, GLOUCESTER POINT, VA 23062, USA

*CORRESPONDING AUTHOR: ashanks@oimb.uoregon.edu

The distribution of the larvae of benthic invertebrates was investigated relative to hydrographic structures as a test of the hypothesis that larvae behave as if they are passive particles. Observations of larval and oceanographic distributions were made off Duck, North Carolina, USA in August 1994. Conditions were characterized by wind-driven coastal upwelling; flow was generally offshore near the surface and onshore below the pycnocline. Within 5 km of the shore the pycnocline was bent upward by the upwelling and it intersected the surface along most of the transects. In zooplankton samples, 20 taxa of larvae were counted (10 bivalve veligers, nine gastropod veligers and one polychaete larvae). Using cluster analysis, larvae were separated into groups with similar patterns of distribution and similar affinities to water properties. The larvae in Cluster 3 did not display a consistent distribution pattern beyond that they tended to be found in warmer surface waters. An earlier paper described the distribution of larvae in the same location during a downwelling event [A. Shanks et al. (2002) J. Plankton Res., 24, 391–416]. Two of the clusters identified during this previous study were quite similar in composition to Clusters 1 and 2 in this study. In both studies, Cluster 1 larvae were found below the pycnocline, but during the upwelling event they were transported shoreward with the advection of the subpycnocline waters by the upwelling circulation. Within 5 km of the shore, Cluster 1 larvae were found at depths shallower than the base of the pycnocline and were often found in patches of high larval concentration. The patches were located where the waters were upwelling. Cluster 2 larvae were found within 5 km of the shore in both studies and tended to be highly concentrated in convergences or divergences. Larvae in Cluster 1 generally appeared to be dispersing as passive particles, except within the zone of upwelling where they may have been swimming against the upwelling flow leading to higher larval concentrations. Cluster 2 larvae appeared to be consistently concentrated in areas of vertical currents, suggesting that they may be attempting to maintain a preferred depth in the face of the vertical flow which would lead to high larval concentration and nearshore larval distributions despite extensive cross-shelf movement of water. Despite their slow swimming speeds, the larvae in Clusters 1 and 2 were not swept offshore by the upwelling event.

INTRODUCTION

Many benthic invertebrates produce larvae that must go through extended periods (days to months) of pelagic development. Mortality is, apparently, generally high during this period (Rumrill, 1990) and variations in mortality are believed to affect subsequent settlement rates at the end of the pelagic development. A potentially important source of mortality may be transport of the larvae away from settlement sites during their pelagic dispersal so that at the end of their development, when they must settle, no suitable habitat is available (e.g. 'larval wastage').

Most invertebrate larvae, especially those reliant on cilia for propulsion, swim much more slowly than the speed of typical horizontal currents (Mileikovsky, 1973; Chia *et al.*, 1984; Young, 1995). Because of this it has been a common assumption that the dispersal of these larvae is at the mercy of the currents; larvae are 'blown' about by the ocean currents as if they were passive particles. If at the end of the pelagic phase they are adjacent to an appropriate settlement habitat then they are simply lucky.

If, however, larvae are not passive but exert some control over the dispersal process, then they may be able to remain in, or be transported to, waters that are in contact with the habitat into which they must settle. Larvae that can control the path of their dispersal may increase their chances of surviving the transition from pelagic larvae to benthic adults.

The data reported here are the results from the 'Coastal Ocean Processes Study' [CoOP'94 (Butman, 1994)]. The purpose of the study was to investigate the nearshore cross-shelf dispersal of invertebrate larvae. During the course of the study, the coastal ocean was dominated by the effects of the local winds. Winds from the northeast generated downwelling against the coast (Cudaback and Largier, 2001) and intrusions into the study area of the Chesapeake Bay estuarine plume (Rennie, 1998). Winds from the south-west generated upwelling flow and the offshore movement and breakdown of the Chesapeake Bay plume by turbulent mixing (Cudaback and Largier, 2001).

In an initial paper we described an extensive set of biological and physical oceanographic data collected on a grid of transects during a downwelling event with the associated intrusion of a plume of Chesapeake Bay estuarine waters (Shanks *et al.*, 2002). We used this data set to test the hypothesis that ciliated invertebrate larvae are dispersed as if they were passive particles. The meroplankton community could be broken down into clusters of organisms with similar distributions. Two clusters composed of just a few taxa were found in small patches; little could be said about their distribution. A third cluster was found predominantly above the pycnocline and a fourth cluster of organisms was most common below the pycnocline. In a time-series of samples collected with a moored plankton pump, Garland *et al.* found a similar association of larvae with water types (Garland *et al.*, 2002). The tight association between the water mass and the larval distributions is consistent with the hypothesis that these larvae were behaving as passive neutrally buoyant particles. We found a fifth cluster that appeared to enter the study grid with the estuarine plume waters. They were tightly coupled to the plume in the more northern transect, but in the transects to the south they were no longer associated with the plume; they were found at greater depths, seaward of the plume in saltier waters. This change in distribution suggests that they may not have been acting as passive particles; by their behaviour they moved from one water mass, the plume water, into an adjacent one. The sixth cluster consisted of organisms that were most abundant in the convergence zone that formed between the plume waters and the downwelling surface layer. Their consistently high concentration in the convergence zone suggests that they were also not acting as passive particles; only actively swimming organisms or buoyant particles can become concentrated in a convergence (Franks, 1992). From this study we concluded that the dispersal of some larval types is consistent with the hypothesis that they are acting as passive particles while other types of larvae exert some control over their dispersal and do not follow the movement of the waters; they were not passive particles.

The work presented here describes sampling that took place during a south-west-wind-generated upwelling event. The area sampled was approximately 30 km alongshore by 20 km offshore, within which sampling was extensive with 27 stations occupied along five transect lines (five or six stations per line). The oceanographic sampling adequately described the vertical shear in the cross-shelf flow associated with the upwelling event and the associated distribution of oceanographic parameters. Concurrent biological sampling allowed us to describe the distribution of meroplankton relative to the oceanography. The sampling provided a second opportunity, under completely different oceanographic conditions, to test the hypothesis that ciliated meroplankton were advected passively by ocean currents. In addition, we could investigate whether weak swimming larvae are swept offshore during upwelling conditions, as is commonly assumed.

METHOD

The fieldwork for this study took place during August 1994. Here we report the results of a grid of stations sampled on August 12–13 during an upwelling event and the offshore movement of the Chesapeake Bay estuarine plume waters. The sampling grid was centred on the Army Corps of Engineers Field Research Facility (FRF) at Duck, North Carolina, USA (Figure 1). This section of coast is characterized by relatively simple submarine and coastal topography. It was hoped that this would minimize topographically induced alongshore variations in the oceanography. Transects were located approximately 20 and 10 km north (transects 3.0 and 3.5, respectively) and 8 and 17 km south (transects 4.5 and 5.0, respectively) of the transect centred on the FRF pier (transect 4.0). Transects were oriented roughly perpendicular to the coast and extended 20 km offshore. Transects 3.0, 4.0, 4.5 and 5.0 had six stations (approximately 1, 2, 4, 9, 14 and 19 km offshore), while transect 3.5 had only five stations (no station at 1 km offshore).

Sampling from the R/V 'Cape Hatteras' began at the most offshore station of transect 3.0 at 19:30 h (GMT) on August 12 and the last station in the grid (transect 5.0, 1 km station) was sampled at 22:55 h (GMT) on August 13. At each station, a SeaBird 911 Conductivity–Temperature–Depth (CTD) cast was made. The

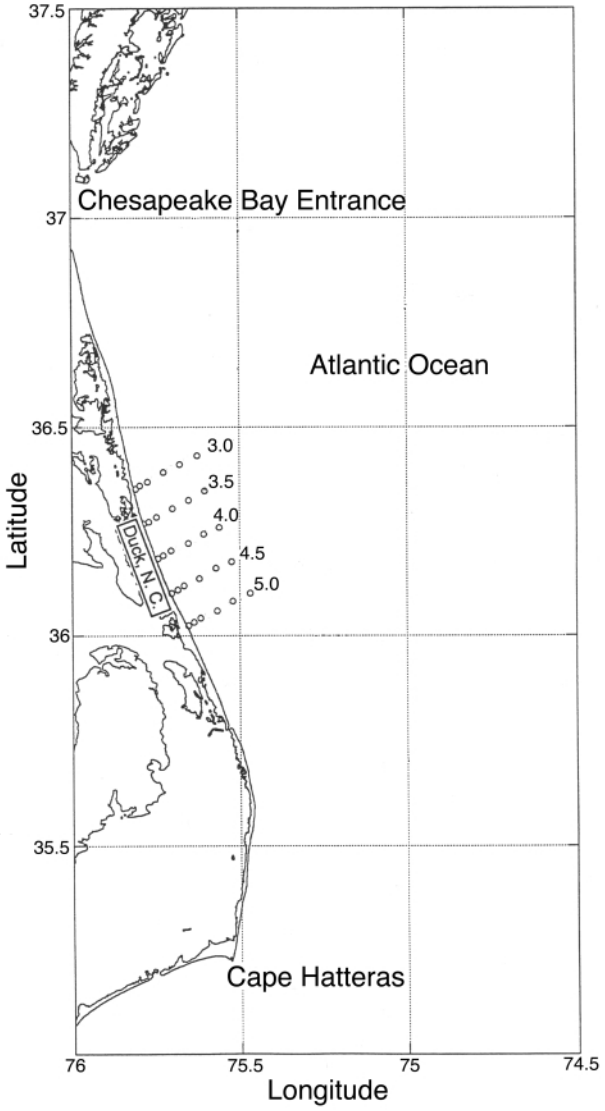

Fig. 1. Map of station and transect locations.

concentration of chlorophyll was measured with a Wet Star *in situ* fluorometer mounted on the CTD. These measurements were not calibrated against extracted chlorophyll samples, hence, the values reported are estimates of the concentration of chlorophyll. The validity of these fluorescence data is discussed further elsewhere (D'Sa *et al.*, 2001). A transmissometer mounted on the CTD was used to measure water clarity. Simultaneous with the CTD cast, an Acoustic Doppler Current Profiler (ADCP) was used to measure the vertical profile of currents. The currents were measured with an RDI 1.2 MHz narrow-band instrument mounted on a catamaran that held the transducer at a depth of 0.4 m. Velocity profiles were made with a vertical resolution of 1 m and recorded at 1–2 Hz while the ship held position for the CTD cast. Surface water temperature and salinity were monitored while the ship was underway. A detailed description of the collection and processing of the physical oceanographic data can be found elsewhere (Waldorf *et al.*, 1995; Rennie, 1998).

Plankton samples were collected with a centrifugal pumping system. A 5 cm diameter hose was connected to the CTD rosette and a deck-mounted pump. Output from the CTD provided information on the depth from which each sample was collected. Water from the pump was passed through a 100 μm mesh net suspended in a large tub of water. The pumping rate was 227 l min^{-1} and 680 l were sampled at each depth. Sampling depths were selected based upon the water depth. At shallow depths (≤20 m) samples were generally collected ~2 m from the bottom, ~2 m from the ocean's surface, and halfway between these samples (Table I). At deeper stations, samples were generally collected ~2 m from the bottom and the surface, within the thermocline, and mid-way between the thermocline and the surface or the bottom (Table I). Samples were preserved in buffered formalin.

In the laboratory, the samples were washed free of formalin on a 53 μm sieve. The sample was transferred to a 250 ml beaker and, with the aid of an electronic balance, was made up to 200 ml (200 g). The sample was then homogenized by vigorous random stirring and a 12 ml sub-sample was removed with a Stempel pipette (Peterson *et al.*, 1979; Omori and Ikeda, 1984). Sub-samples were counted until at least 100 individuals of the most common organisms had been enumerated. This yielded a sample standard deviation of ~10% for the most abundant organisms and between 10 and 20% for the less common species (Venrick, 1978). To test the sub-sampling technique, we compared the number of organisms in four samples determined by sub-sampling and by counting the entire sample. No statistically significant differences (Mann–Whitney U test, $P > 0.05$) were found between the number of organisms determined by the two methods, indicating that the sub-sampling technique adequately described the samples.

The plankton samples were sorted under a dissecting microscope equipped with polarizing filters placed between the sample and the light source and between the sample and the microscope lens. The filters were rotated until the shells of bivalves and gastropods appeared to 'glow' because of the birefringence caused by the crystalline structure of the shell (Gallager *et al.*, 1989). Lighting the samples in this way greatly facilitated sorting. Bivalve and gastropod larvae were identified to genus and, when possible, to species using various identification guides (Thorson, 1946; Sullivan, 1948; Rees, 1950; Loosanoff *et al.*, 1966; Chanley and Andrews, 1971; Thiriot-Quievreuz, 1980; Gallager *et al.*, 1989). Polychaete larvae

Table I: Depth (m) of plankton samples and station locations within the transect grid

Station no. (distance alongshore)	Offshore distance of stations (km)					
	1 km	2 km	4 km	9 km	14 km	19 km
3.0 (0 km)	2	2	2	2	2	2
	5	6	7	10	7	5
	8	10	15	15	11	8
					16	15
					20	22
3.5 (10 km)		2	2	2	2	2
		7	6	8	8	8
		12	15	14	14	14
				16	17	24
					21	22
4.0 (20 km)	2	2	2	2	2	2
	6	9	8	6	7	7
			15	10	12	12
			19	15	17	24
				19	23	
4.5 (28 km)	2	2	2	2	2	2
	8	8	6	7	7	6
		14	10	13	12	11
			15	16	16	17
				20	20	23
5.0 (37 km)	2	2	2	2	2	2
	5	10	5	10	9	8
	8	13	8	16	16	14
			13		20	18
			18		25	23

were identified to family using descriptions in Thorson and in Bhaud and Cazaux (Thorson, 1946; Bhaud and Cazaux, 1982).

During the processing of the physical oceanographic data, current velocities were decomposed into alongshore and cross-shore components. Alongshore was defined as 20°W of true North. Contour plots of the distribution of the biological and physical data were made using the Noesys Transform contour plotting program with the Kriging option for gridding and interpolating. In these plots, the positions of contours close to shore (within 5 km), because of the short distance between stations, are probably depicted fairly accurately. Station spacing increased with distance offshore and the confidence in the continuity of distributions between stations decreased. While station spacing was chosen based on the idea that cross-shore decorrelation length scales for physical variables are longer than station spacing (both increasing offshore), decorrelation length scales for meroplankton distributions are not known and they are not necessarily so large. Hence, the contour plots of larval distributions must be interpreted with some caution.

RESULTS

Oceanographic distributions

In the following presentation, the results and their interpretation in the discussion section are presented as a 'snap shot' of the conditions during the sampling cruise. The data actually took about a day to collect, during which time the water in the study area was, of course, in motion. Alongshore currents, particularly nearshore, were 20–40 cm s^{-1}, rapid enough to move a parcel of

water 20–40 km northward during the time it took to sample the grid of transects. This is a problem shared by nearly all physical and biological oceanographic sampling surveys.

Upwelling-favourable winds from the south-west commenced on the evening of August 11 at about 22:00 h and continued to blow until August 15. Thus upwelling winds commenced ~24 h before the beginning of the sampling reported here.

The effects of the upwelling-favourable winds can be clearly seen in the distribution of temperature along the transects (Figure 2). Along each transect the isotherms in the thermocline (temperatures between about 22 and 17°C) tilt upward near the coast. The upward tilt of the thermocline starts within about 5 km of shore and, in all but transect 3.5, the thermocline intersects the surface. Seaward of 5 km, the isotherms of the thermocline are relatively horizontal. The warmest waters in the study area were found at the most seaward edge of the transects. Within and below the thermocline, variations in density appeared to be primarily the result of variations in temperature.

During downwelling-favourable winds, the estuarine plume from the Chesapeake Bay enters the study area as a narrow, rapidly flowing water mass pressed up against the shore (Rennie *et al.*, 1999). With the onset of upwelling-favourable winds, the plume separates from the coast and moves offshore as a thin lens of low-salinity water that mixes with the surrounding shelf waters (Rennie, 1998; Cudaback and Largier, 2001). The remains of the Chesapeake Bay plume waters are most obvious in transect 3.0 (Figure 3). Here, centred about 5 km from shore, we see a lens of water with salinity as low as 29.5 p.s.u. In each of the transects to the south, we see remnants of the Chesapeake Bay plume in the form of thin (several metres thick) lenses of low-salinity water separated from the shore (Figure 3). The salinity in these more southern extensions of the plume remained above 30 p.s.u. These salinity variations are mostly in the upper 10 m and it is these salinity structures that dominate density structure above the thermocline.

Inspection of Figures 2 and 3 and the associated temperature/salinity diagram (Figure 4) suggests that there were three water masses in the study area. (i) Chesapeake Bay-influenced waters: the relatively warm (>22°C) and lower salinity (<31 p.s.u.) near-surface waters are the remnants of the Chesapeake Bay estuarine plume that have been advected offshore through upwelling and are mixing with the shelf surface waters. (ii) Gulf Stream-influenced outer shelf waters: the relatively warm (>19°C) and higher salinity near-surface water (>32 p.s.u.) found further offshore is in part composed of Gulf Stream waters that have moved onto the shelf (Cudaback and Largier, 2001). (iii) Middle Atlantic Bight shelf waters: these waters are represented by the relatively linear relationship between cool salty sub-thermocline and warm low-salinity near-surface and thermocline waters (Cudaback and Largier, 2001).

Alongshore flow within 5 km of shore was consistently to the north, at speeds of ~10–30 cm s^{-1}. Beyond 5 km from shore, alongshore flow was more variable. Cross-shelf flow was predominantly seaward above the thermocline (Figure 5) and landward below, a flow pattern indicative of upwelling. Transect 4.0 was an exception to this general pattern. Along this transect, cross-shelf flow was almost entirely onshore and stronger above the thermocline. It should be noted, however, that despite this flow pattern, one that is more indicative of a downwelling regime, the temperature isotherms (Figure 2) clearly indicate an upwelling pattern. Typically in upwelling systems, areas of offshore surface flow (e.g. transects 3.0 and 5.0) are separated by areas of weaker offshore or even onshore flow (e.g. transect 4.0) (Kosro and Huyer, 1986; Kosro *et al.*, 1997).

Inspection of Figure 5 suggests that above the thermocline there were zones of convergence and divergence in the cross-shelf flow. We calculated the strength of the divergence in cross-shelf flow ($\delta u/\delta x$) from the interpolated velocity field $u(x, z)$ shown in Figure 5; where u is cross-shelf, x is cross-shelf distance, z is depth; and $\delta u/\delta x$ is calculated as $\Delta u/\Delta x$ using a centre-difference value for the gradient at each grid point (x, z). This flow divergence is plotted in Figure 6, with positive values indicating zones of divergence and negative values indicating zones of convergence.

Along each transect, relatively strong convergences (~–1 s^{-1}) and divergences (around 1.0 s^{-1}) were found within 5 km of shore (Figure 6). Seaward of 5 km, convergences and divergences were generally weak, with values between 0.5 and –0.5 s^{-1} (Figure 6). While we would expect higher values in the zone of upwelling, it should be noted that the larger station spacing offshore would smooth out any localized high-gradient regions that may exist offshore (ADCP data are only available at station locations). Along transects 3.0, 3.5 and 4.5, immediately adjacent to shore the flow fields were convergent with a switch to a divergent flow field at ~4–5 km from shore. Along transects 4.0 and 5.0, the flow fields next to shore were divergent. Along transect 4.0, the divergence was relatively weak (peak value of 0.4 s^{-1}) and flow switched to a strong convergence (peak value of –1.0 s^{-1}) at ~3 km from shore. On transect 5.0, the divergence next to shore was relatively strong (peak value of 2.0 s^{-1}) and extended offshore to about 3 km, beyond which the flow field was weakly convergent.

Note that the ADCP current data were not 'de-tided'.

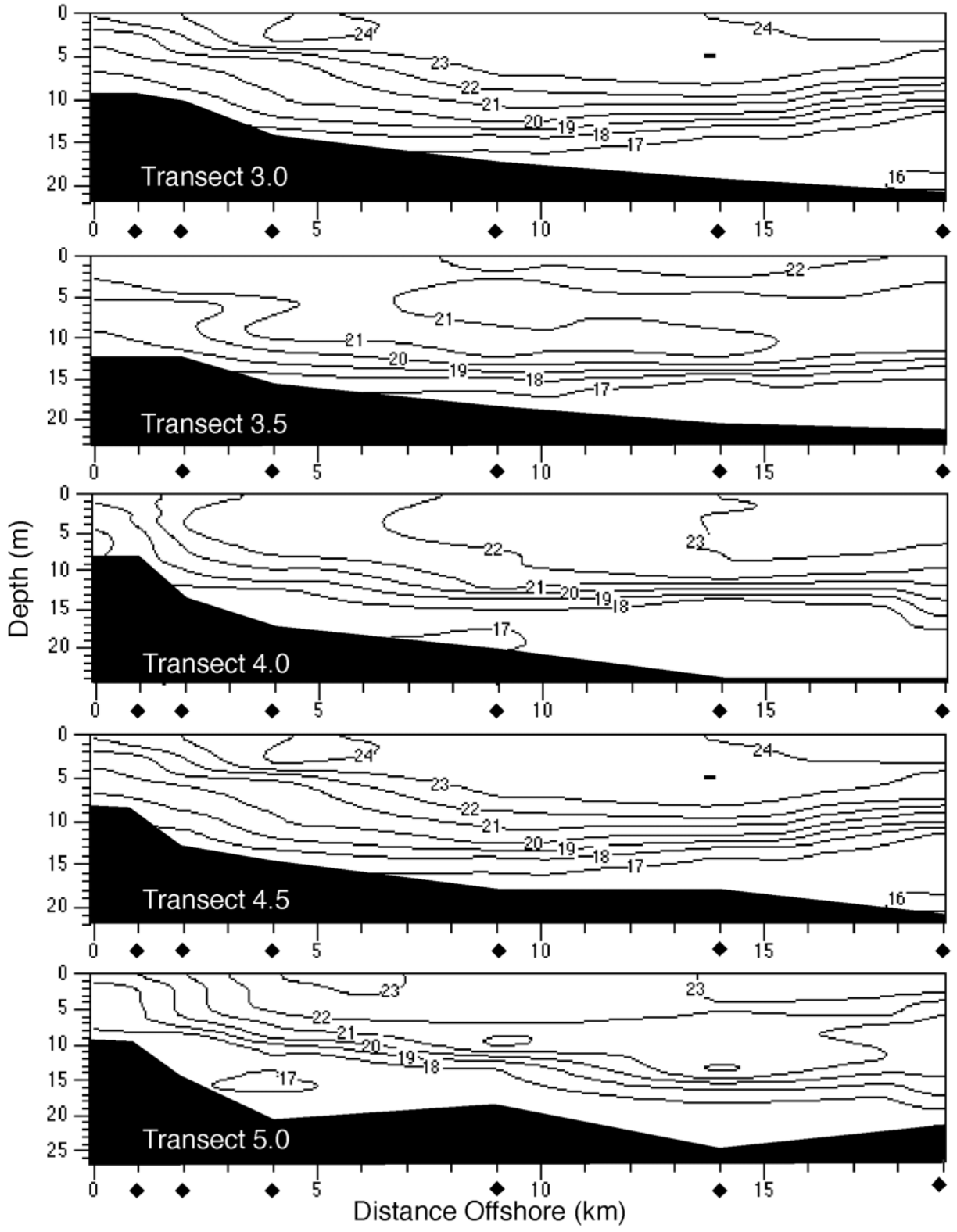

Fig. 2. Contour plots of temperature (°C) along the transect lines. The black diamonds along the horizontal axes indicate station locations.

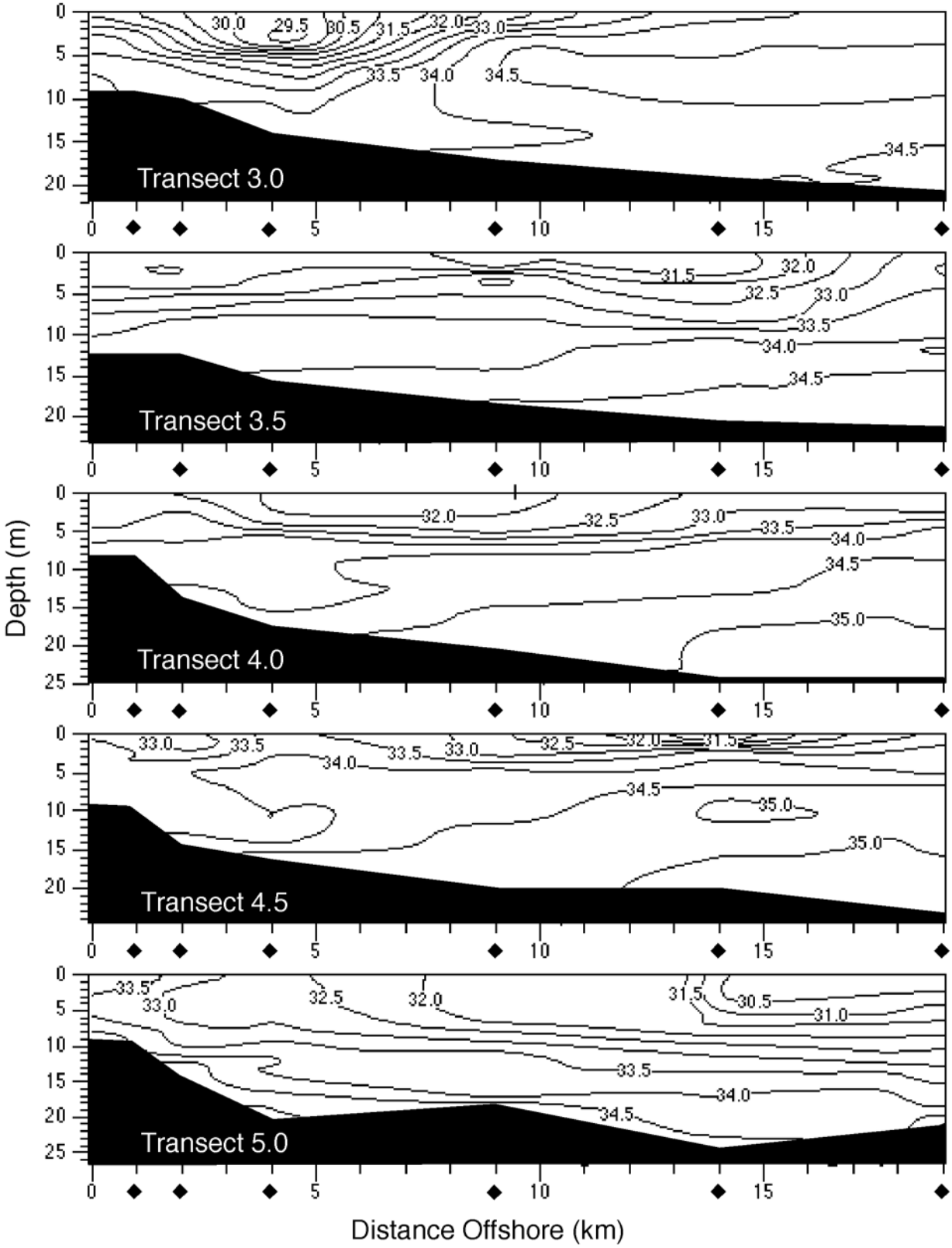

Fig. 3. Contour plots of salinity (p.s.u.) along the transect lines. The black diamonds along the horizontal axes indicate station locations.

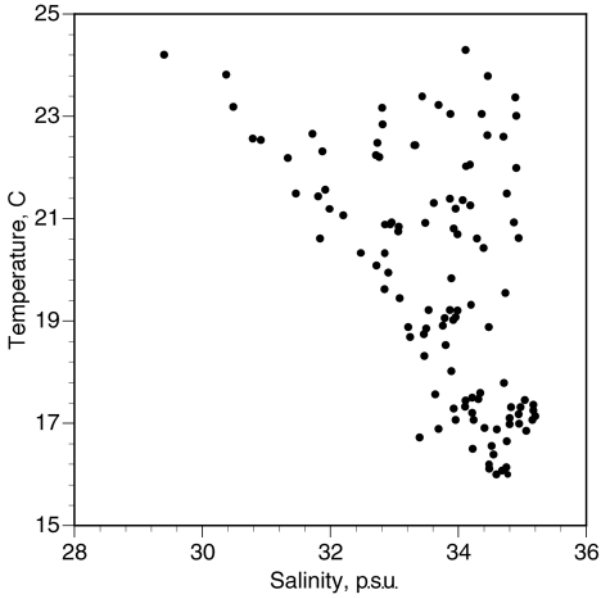

Fig. 4. Temperature/salinity diagram of the waters in the study area. The values are plotted from all of the CTD casts (average value from each metre depth interval).

The tidal currents, however, were relatively small (Lentz *et al.*, 2001): the M2 tide was the strongest constituent and the amplitude varied over the survey with alongshore M2 velocities increasing from 3 cm s^{-1} at the coast to 5 cm s^{-1} at the seaward end of the transects. Cross-shelf tidal velocities varied from 0 to ~3 cm s^{-1} at the coast and the seaward end of the transects, respectively. The cross-shelf gradients in the tidal currents were thus very small, negligible compared with the observed convergences and divergences.

In general, per cent light transmission (m^{-1}) was lower below the thermocline and close to the bottom (Figure 7). On transects 3.0, 3.5, 4.0 and 4.5 the areas of lowest light transmission were found within 2 km of the coast in waters that were in the process of being upwelled. On transect 5.0 there was no such pattern of near-bottom turbidity associated with upwelling. Here the waters with the lowest per cent transmission were found at the surface, above the thermocline, and ~3–6 km offshore.

Below the thermocline, chlorophyll concentrations were generally very low (Figure 8). Above the thermocline, chlorophyll concentrations were also generally low, but with distinct patches of higher chlorophyll concentration. Nearshore (within 5 km of shore) there were patches of higher chlorophyll concentration present along each transect. Along transects 3.0 to 4.5, this nearshore patch appeared to be associated with the nearshore convergence zones (compare Figures 6 and 8). Along transect 5.0, the nearshore chlorophyll patch was associated with the nearshore divergence zone (compare Figures 6 and 8). The relationship between the nearshore patches of high chlorophyll concentration and convergence or divergence suggests that these patches may be the result of mechanical concentration of the phytoplankton. Offshore patches of higher chlorophyll concentration were also found on transects 3.5, 4.0 and 5.0. On transects 3.5 and 5.0, the offshore patches of higher chlorophyll abundance appeared to have been associated with lenses of lower salinity surface water (compare Figures 3 and 8), but this was not so on transect 4.0.

Larval concentration

We counted a total of 11 975 bivalve larvae. We were able to identify 10 different bivalve genera or species in our samples. No larval type accounted for more than 17% of the total abundance of bivalve larvae. Approximately 13% of the bivalve larvae could not be identified. We did not attempt to identify the early developmental stages of larval bivalves (the so-called D-stage larvae). Probably because of our use of 100 μm mesh nets, very few D-stage larvae were caught.

A total of 6198 gastropod larvae were counted, from nine genera. Two genera, *Lacuna* sp. and *Hydrobia* sp., accounted for 38% of the catch. Approximately 26% of the gastropod larvae could not be identified.

We counted a total of 1137 polychaete larvae from three families, Spionids, Magellonids and Phyllodocids. More than 90% of the polychaete larvae enumerated were Spionids. Because Magellonids and Phyllodocids were uncommon we did not include them in the following analysis. Trochophores were not common and were not counted.

Here we describe the distribution of 20 taxa. They were sorted into groups using the Cluster Analysis statistical package in Statistica™. Two different techniques were used. The first technique separated larvae into groups based on their spatial distribution. The concentrations of larvae were standardized such that the mean was equal to 0 and the standard deviation was equal to 1 (StatSoft, 1994). Using the Wards method, the larvae were grouped into clusters by their Euclidean distance. This analysis (as well as several of the other clustering algorithms) suggested that the larvae could be placed in three clusters (Figure 9, numbered clusters). The second technique formed clusters based on the relative affinity of larvae to location or water type. Correlations were calculated between larval concentrations and the physical variables (temperature, salinity, alongshore velocity, cross-shore velocity, offshore distance, alongshore distance, per cent light transmission and depth) and chlorophyll concentration. This correlation matrix was then used in the cluster analysis. Using the Wards method, the larvae were

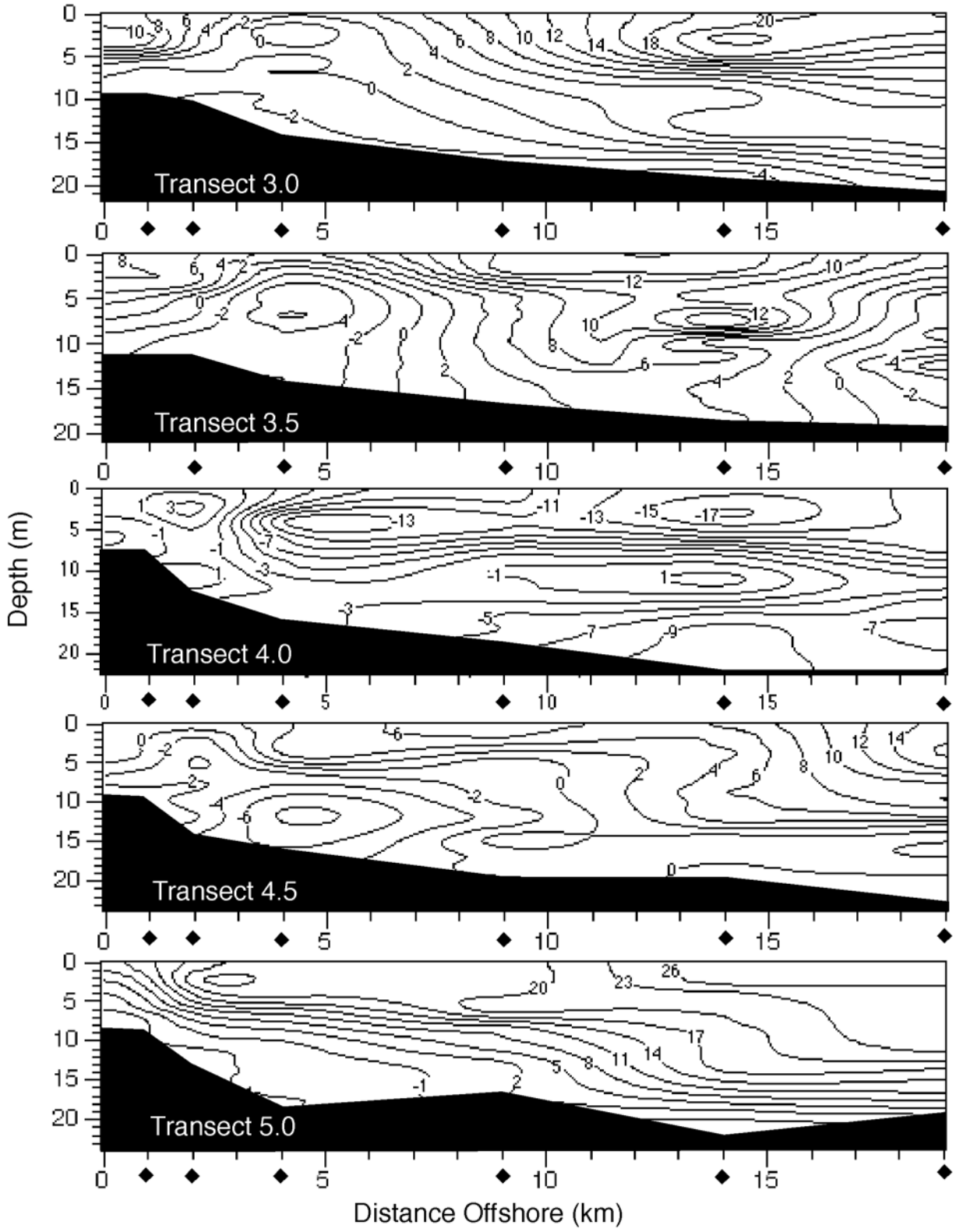

Fig. 5. Contour plots of cross-shore flow (cm s^{-1}) along the transect lines. Negative values indicate onshore flow. The black diamonds along the horizontal axes indicate station locations.

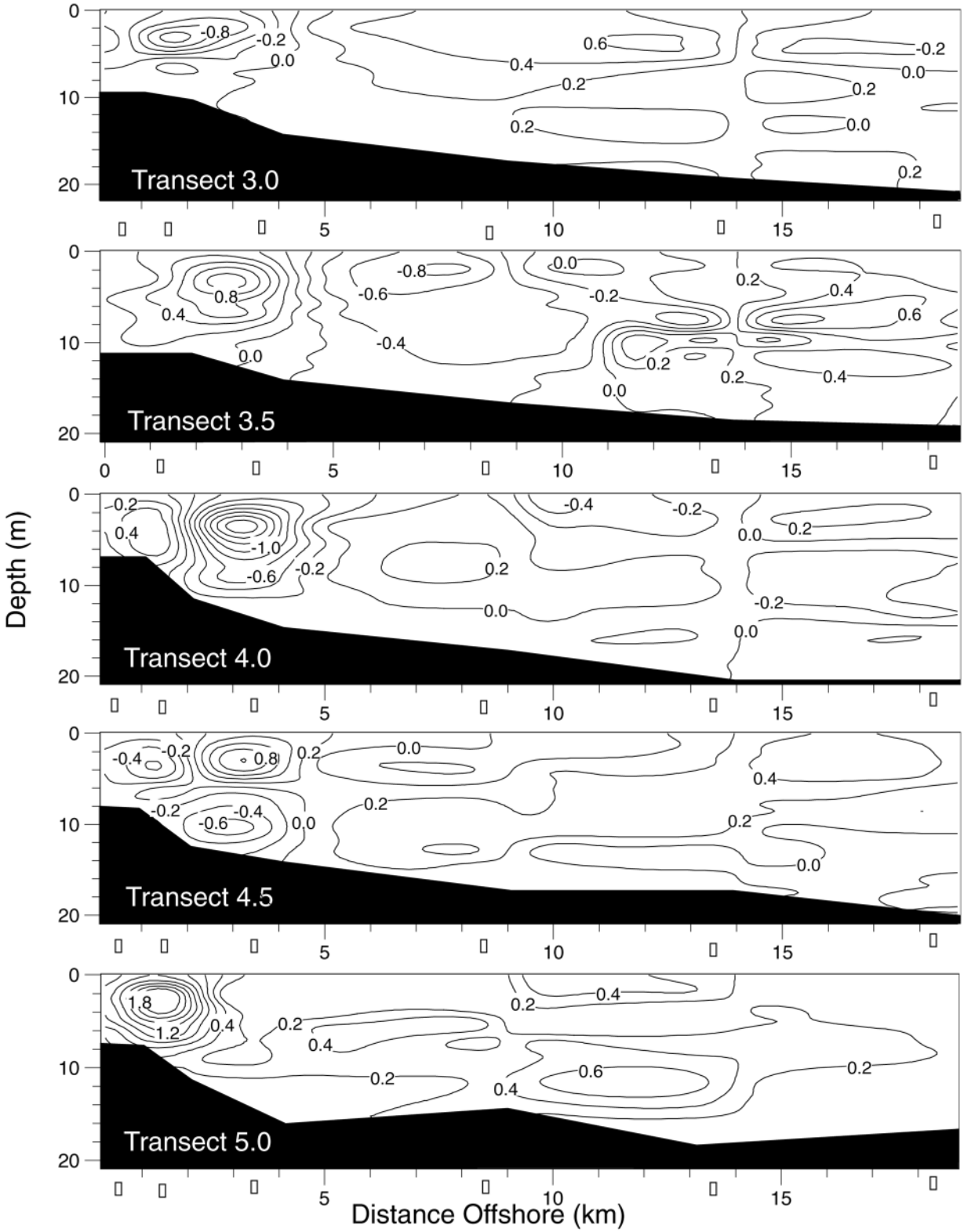

Fig. 6. Contour plots of cross-shore velocity divergence (s^{-1}) along the transect lines; zones of divergence and convergence have positive and negative values, respectively. See the text for a description of the methods used to calculate these values. The black diamonds along the horizontal axes indicate station locations.

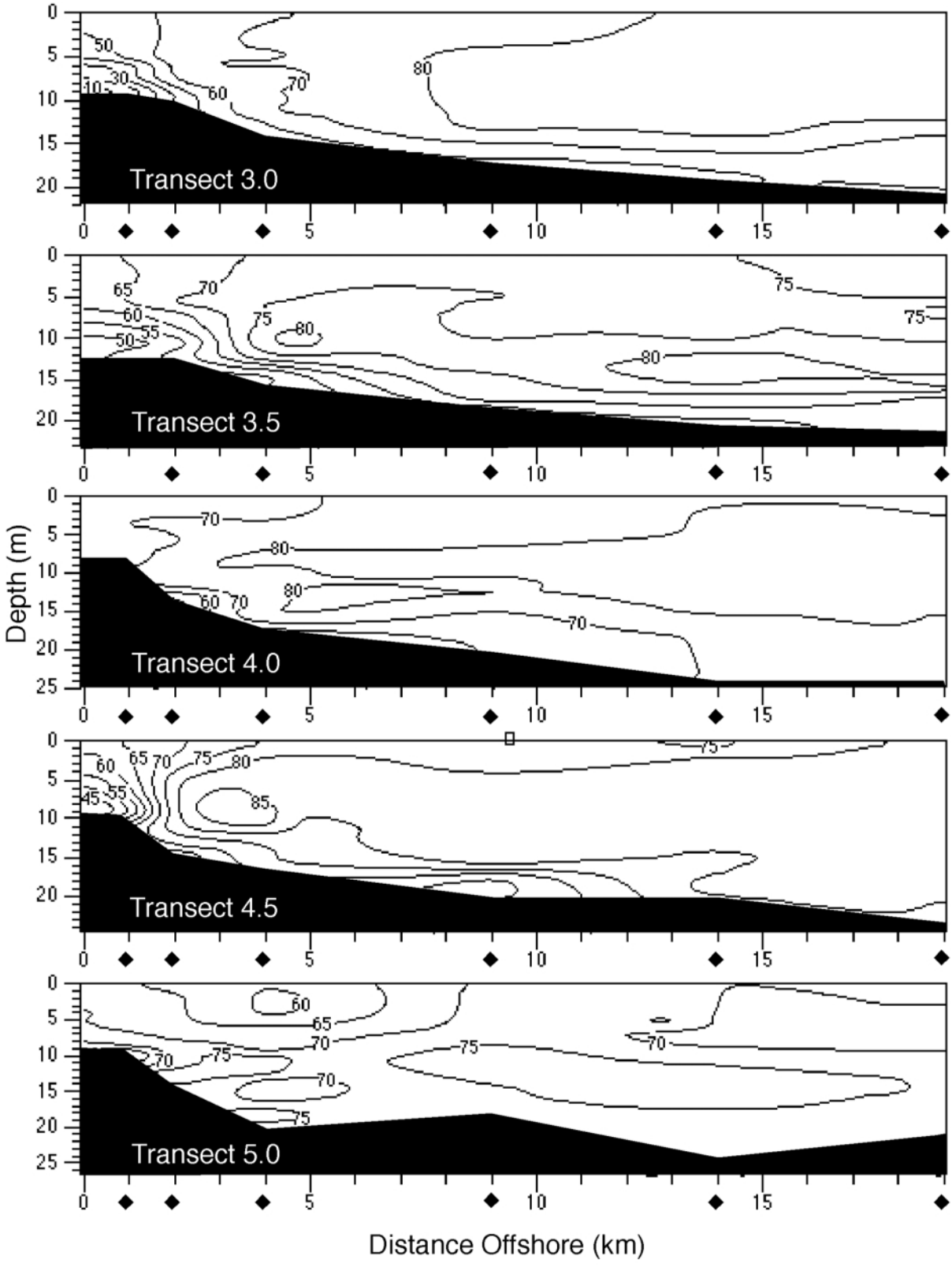

Fig. 7. Contour plots of per cent light transmission (m^{-1}) along the transect lines. The black diamonds along the horizontal axes indicate station locations.

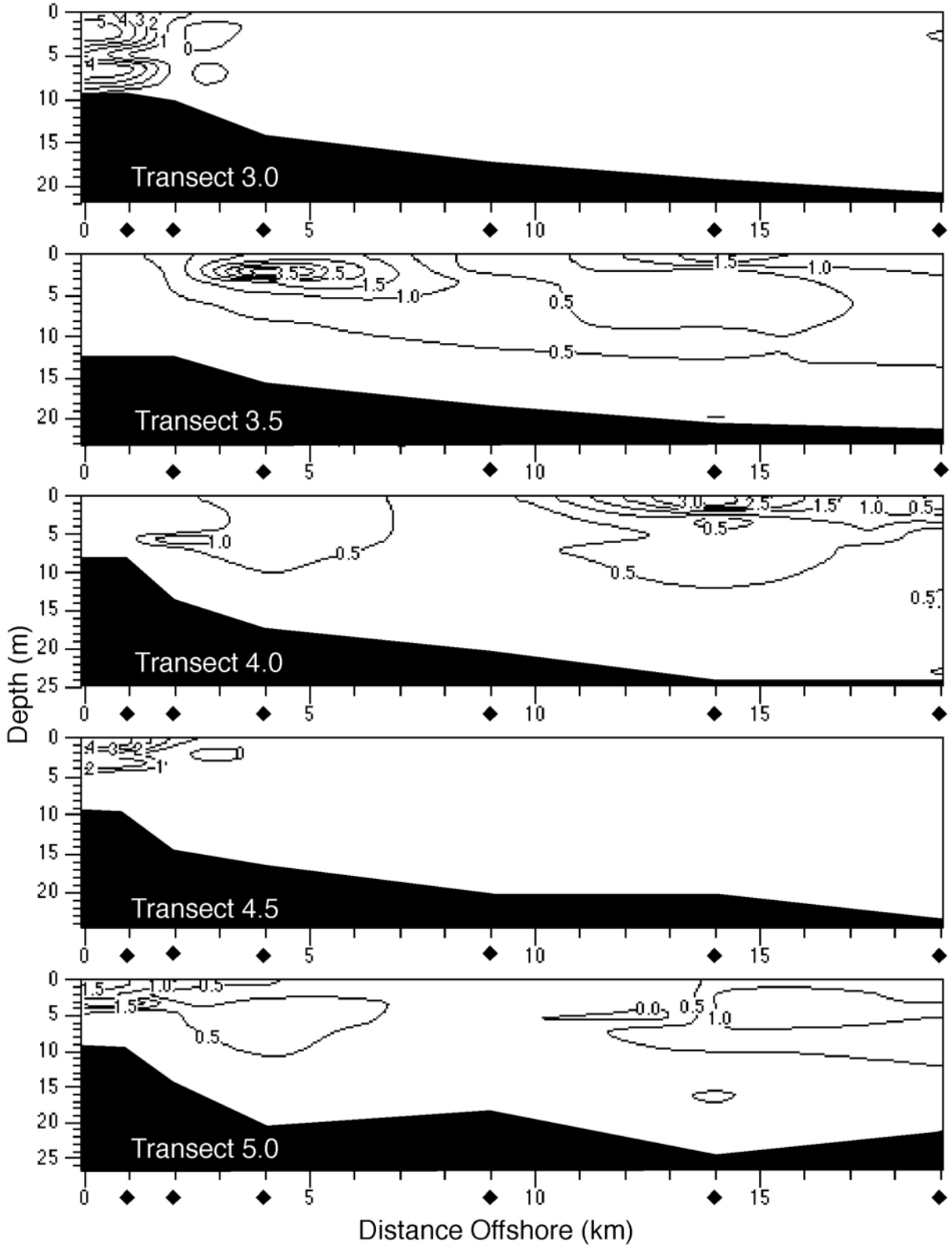

Fig. 8. Contour plots of chlorophyll fluorescence (uncorrected values, μg l^{-1}) along the transect lines. The black diamonds along the horizontal axes indicate station locations.

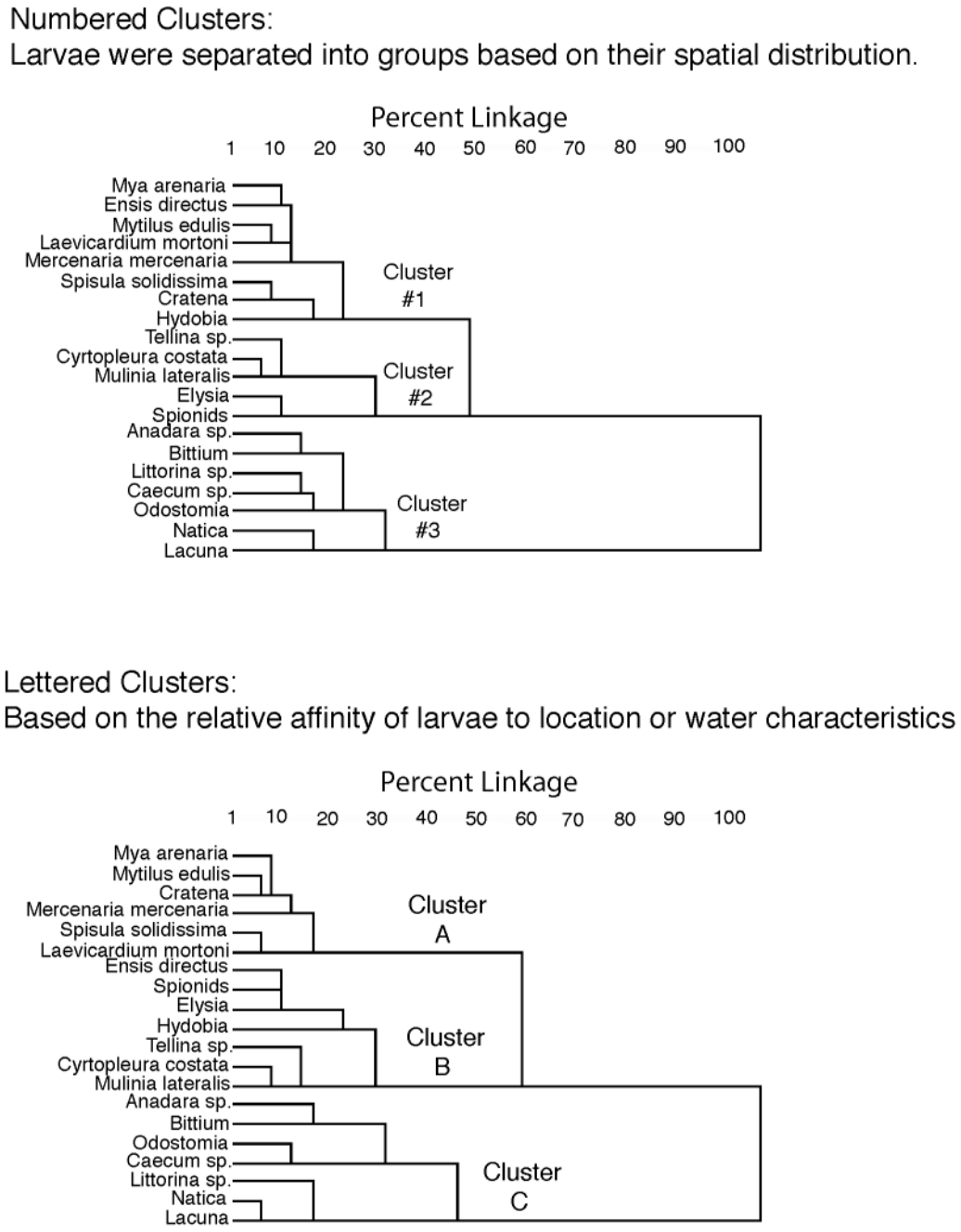

Fig. 9. Results of cluster analyses that separated larvae into groups based on their spatial distribution (Numbered Clusters) and the relative affinity of larvae to location or water type (Lettered Clusters). Per cent linkage is the minimum linkage distance divided by the maximum linkage distance multiplied by 100. For the determination of the Numbered Clusters, the concentrations of larvae were first standardized such that the mean was equal to 0 and the SD was equal to 1 and then using the Wards method the larvae were grouped into clusters by their Euclidean distance. For the determination of the Lettered Clusters, correlations were calculated between larval concentrations and the physical variables (temperature, salinity, alongshore velocity, cross-shore velocity, offshore distance, alongshore distance, per cent light transmission and depth) and chlorophyll concentration. This correlation matrix was then used in the cluster analysis. Using the Wards method, the larvae were grouped into clusters by their correlation coefficients with the physical variables and chlorophyll concentration.

grouped into clusters by their correlation coefficients with the physical variables. This analysis also indicated that there were three clusters (Figure 9; lettered clusters).

The two different analyses generated almost identical clusters. Cluster 3 and Cluster C were composed of the same set of taxa. Clusters 1 and 2 were quite similar to Clusters A and B, respectively. In the numbered clusters, *Hydrobia* sp. and *Ensis directus* were included in Cluster 1, but in the lettered clusters they were included in Cluster B. About 90% of the larvae that composed the numbered clusters were found in lettered clusters composed of similar members. Given the strong similarity between the clusters generated by the different analyses we will concentrate the following presentation of the results on the numbered clusters.

Cluster 1

Cluster 1 was composed of eight taxa, *Mya arenaria*, *Ensis directus*, *Mytilus edulis*, *Laevicardium mortoni*, *Mercenaria mercenaria*, *Spisula solidissima*, *Cratena* sp. and *Hydrobia* sp. (Figure 9 and Table II). Organisms in this cluster were moderately abundant (concentrations up to several hundred m^{-3}) and were present at all stations in the transect grid. They tended to be more abundant deeper in the water column and below the pycnocline, as indicated by the significant positive correlations with depth, salinity and density and the significant negative correlation with temperature. The significant negative correlations with distance offshore indicated that they tended to be more abundant closer to shore. Temperature/salinity bubble diagrams (Figure 10) can be used to characterize the water mass with which Cluster 1 organisms were associated. Small bubbles (low concentrations) were found in the Chesapeake Bay plume water type (warm, low-salinity water) and in the Gulf Stream water type (warm, high-salinity water). The largest bubbles (highest concentrations) were found in the shelf waters and at lower temperatures and higher salinities; a position on the temperature/salinity curve indicative of a tendency towards a sub-thermocline distribution.

The distribution of *M. arenaria* will be used as an example of the pattern of distribution of organisms in this cluster (Figure 11). The bulk of the *M. arenaria* larvae were found below the thermocline. Beyond ~5 km from shore, the upper limit of their distribution appeared to have been set by the bottom of the thermocline. Within 5 km of the coast, the larvae were found at shallower depths and in association with the upwelling of the thermocline and sub-thermocline waters. Along transects 3.0, 3.5 and 5.0 there were patches of higher larval concentration (>200 m^{-3}) superimposed on a general background concentration of 50–100 m^{-3} (a patch was defined as the mean concentration + one standard deviation, i.e. >200 m^{-3}). No patches with larval concentration much higher than background were found along either transect 4.0 or 4.5. Along the five transects, there were five patches of high *M. arenaria* concentration; two of these patches were found adjacent to shore in association with the upwelled waters and the remaining three were found offshore and below the thermocline. This was a typical pattern of patch distribution for the organisms in this cluster. There were 59 patches of Cluster 1 larvae, of which 24 were found within the upwelled nearshore waters and the remainder were offshore below the thermocline.

Cluster 2

Cluster 2 was composed of five taxa, *Tellina* sp., *Cyrtopleura costata*, *Mulinia lateralis*, *Elysia* sp. and spionid polychaetes (Figure 9 and Table II). Organisms in this cluster tended to be slightly more abundant than those in Cluster 1, with concentrations up to >1000 m^{-3}, and were present at all or nearly all stations (Table II). Organisms in this cluster tended to be more abundant at the northern end of the grid and closer to shore (significant negative correlations with distance both along- and cross-shore; Table II). In addition, they all tended to be found at higher concentrations where the per cent transmission of light was lower (significant negative correlations with per cent light transmission; Table II). This was the strongest correlation between the abundance of these taxa and the various physical variables. The waters with lower light transmission were all found close to shore in areas where upwelling was occurring (Figure 6). In the temperature/salinity bubble diagrams (Figure 12) small bubbles (low concentrations) were generally found in the Chesapeake Bay plume water type (warm, low-salinity water) and in the Gulf Stream water type (warm, high-salinity water). The largest bubbles (highest concentrations) were found in the shelf waters.

The distribution of *Tellina* sp. will be used as an example of the distributions of the organisms in Cluster 2 (Figure 13). Along each transect, the highest concentration of *Tellina* sp. larvae was found within 5 km of shore in waters that were being upwelled. The tight association between upwelled waters and high larval concentrations is a pattern seen throughout this cluster. Amongst the five taxa that comprised Cluster 2, there were 26 patches of larvae (patch concentration = mean concentration + one standard deviation). Twenty were found within 5 km of shore in the upwelled waters. As seen in the distribution of *Tellina* sp., most of these patches were found immediately adjacent to shore. Of the six patches that were found offshore, five were found in the distribution of *Elysia* sp.

Table II: Organisms in numbered and lettered clusters

Taxa	Cluster letter	% Stations present (range, no. m^{-3})	Along shore distance	Cross-shore distance	Depth	Cross-shore flow	Along shore flow	Salinity	Density	Temp.	Per cent light transmission
Cluster 1											
Mya arenaria	A	100 (0–490)		0.3266				0.3011	–0.4583	–0.2188	
Ensis directus	B	100 (0–206)	–0.3159	0.1885					–0.3419	–0.3068	
Mytilus edulis	A	100 (0–552)		0.3784			0.2009	0.3678	–0.4992		
Laevicardium mortoni	A	100 (0–247)	–0.1970	0.2570				0.2579	–0.4050		
Mercenaria mercenaria	A	100 (0–338)		0.4342			0.2627	0.4047	–0.4879		
Spisula solidissima	A	100 (0–988)	0.2472	–0.2339				0.2289	–0.3497		
Cratena sp.	A	100 (0–363)	–0.2237	0.4077			0.2040	0.3676	–0.4962	–0.2026	
Hydrobia sp.	B	100 (0–499	–0.2163			–0.2214	–0.2289			–0.2436	
Cluster 2											
Tellina sp.	B	100 (0–988)	–0.2664	–0.4972				–0.2300			–0.6299
Cyrtopleura costata	B	100 (0–1334)	–0.2543	–0.3585							–0.4136
Mulinia lateralis	B	96 (0–1045)	–0.2012	–0.2450							–0.3296
Elysia	B	100 (0–173)	0.1863		0.2339				0.2246	–0.3128	–0.3848
Spionids	B	100 (0–947)		–0.3849						–0.3203	–0.5945
Cluster 3											
Anadara sp.	C	100 (0–321)		–0.2283	–0.4307			–0.4951	–0.4898	0.3443	
Bittium sp.	C	71 (0–247)	0.2412		–0.2221			–0.2249	–0.2825	0.2810	
Littorina sp.	C	100 (0–181)						0.1905			
Caecum sp.	C	100 (0–189)								0.2861	
Odostomia	C	88 (0– 315)	–0.2981		–0.2887	–0.3095	–0.3284			0.3969	
Natica	C	71 (0–615)	0.3427	–0.2588							
Lacuna	C	96 (0–617)	0.3567								

The percentage of the stations where these organisms were caught and the range in concentration (no. m^{-3}) are presented in column 3. The remaining columns in the table present the results of correlations between the concentration of an organism and the physical variables. Only significant ($P < 0.05$) r values are presented, therefore there is no column for chlorophyll fluorescence.

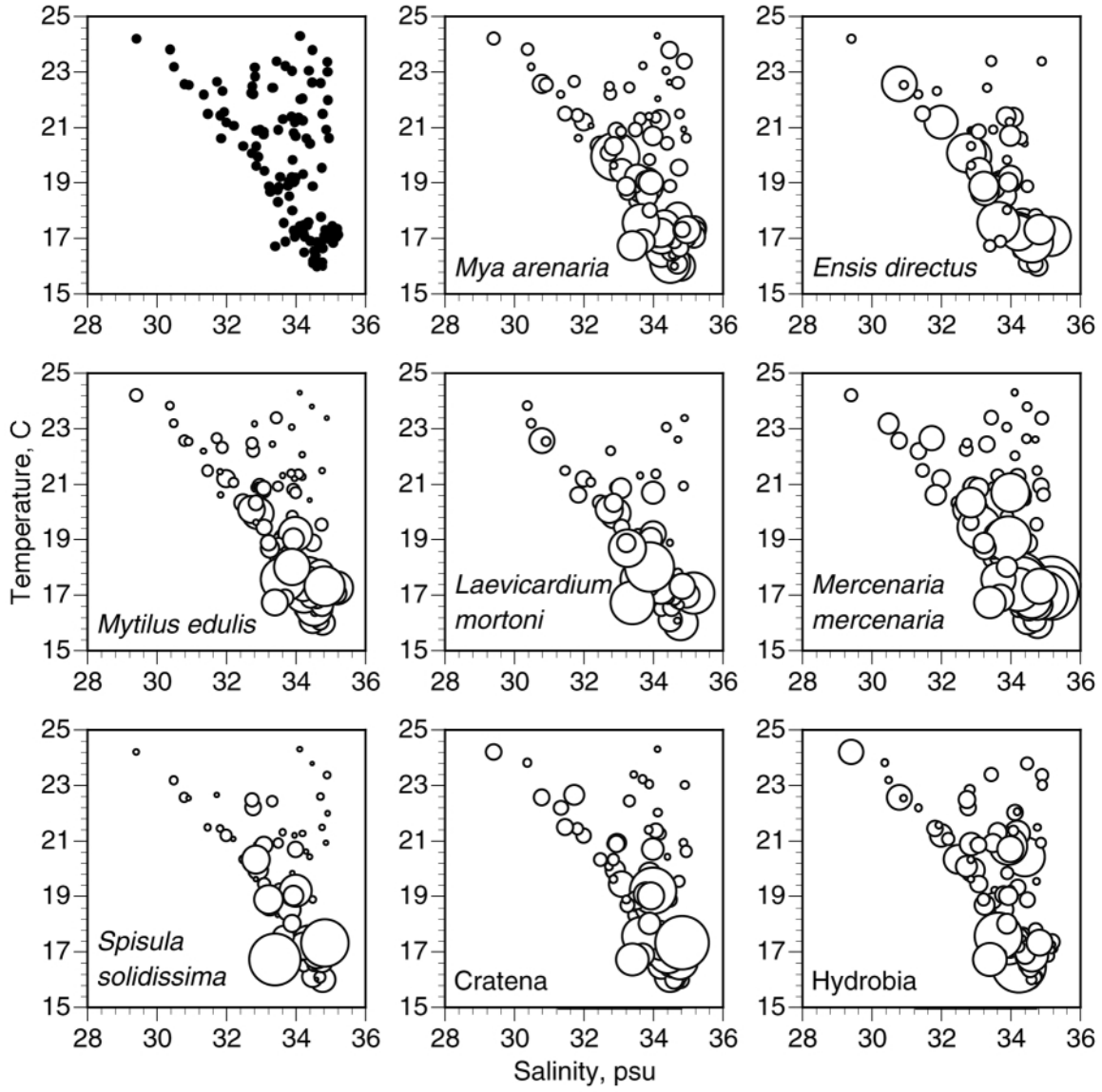

Fig. 10. Temperature/salinity diagram describing the relationship between temperature and salinity of the water in the study area, and temperature/salinity bubble diagrams describing the relationship between the temperature and salinity of the water and the concentration of larvae in Cluster 1 in those waters. The size of the bubble is proportional to the concentration of larvae.

Cluster 3

Cluster 3 (Figure 9) was composed of one bivalve taxon, *Anadara* sp., and six gastropod taxa: *Bittium* sp., *Littorina* sp., *Caecum* sp., *Odostomia* sp., *Natica* sp. and *Lacuna* sp. These organisms were moderately abundant (hundreds m^{-3}) and were present at 70–100% of the stations (Table II). The relationship between the physical variables and the distribution of the taxa in this cluster is not as clear as in the previous two clusters. The most consistent pattern is that the concentrations of four of the seven taxa were significantly positively correlated with temperature (Table II). This relationship can be seen in the temperature/salinity bubble plots (Figure 14). The largest bubbles (highest concentrations) tended to be found in either the warmer, higher salinity waters that were of Gulf Stream origin (*Littorina* sp., *Caecum* sp., *Odostomia* sp., *Natica* sp. and *Lacuna* sp.) or in warmer, lower salinity waters that were part of the Chesapeake Bay plume (*Anadara* sp., *Bittium* sp.). Because of the lack of a general pattern to the distribution of these taxa we will not present a representative taxa as an example.

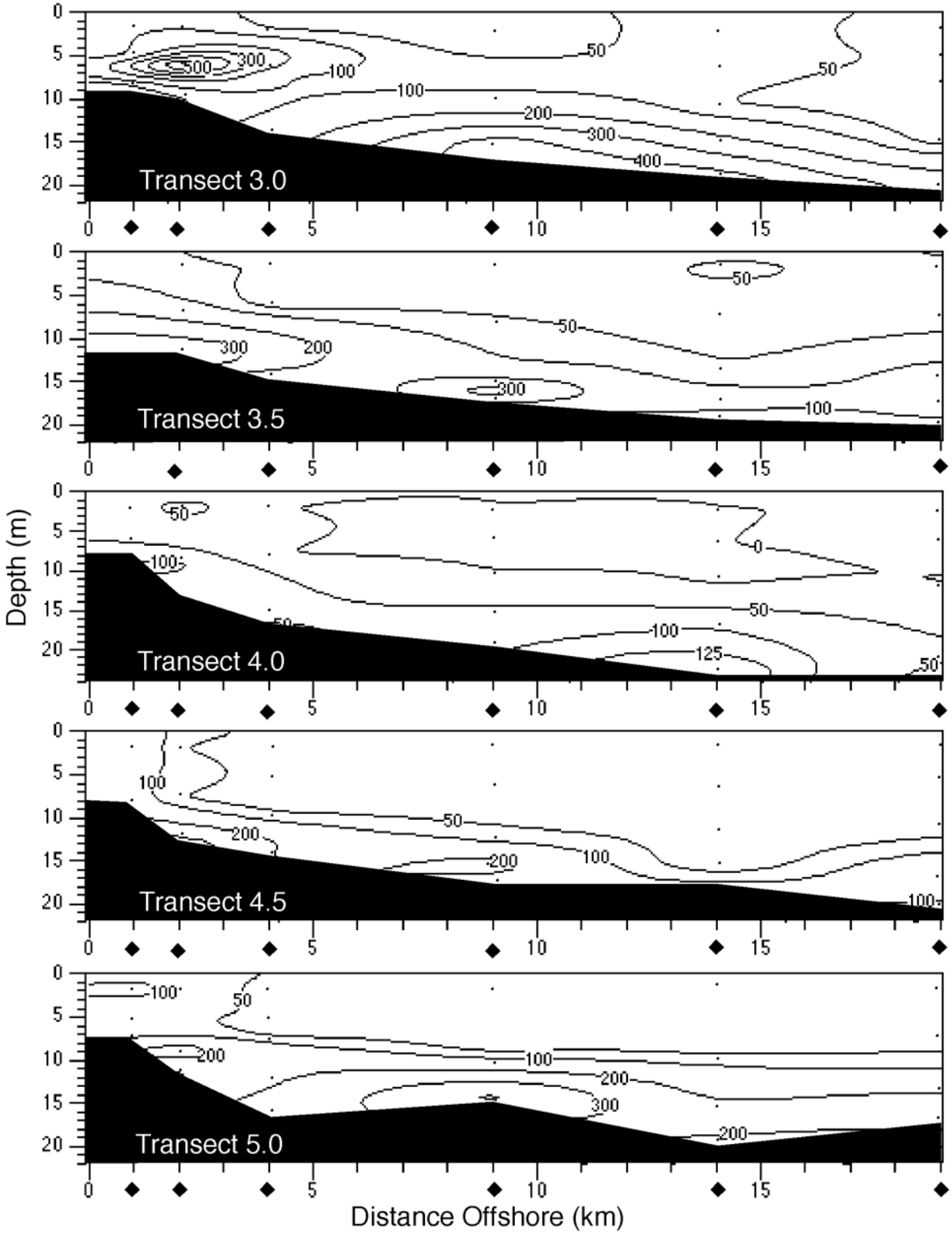

Fig. 11. Contour plots of *Mya arenaria* concentrations (no. m^{-3}), an example of a Cluster 1 or Cluster A larva, along each of the transect lines. The black diamonds along the horizontal axes indicate station locations. Sample depths are indicated by the small dots.

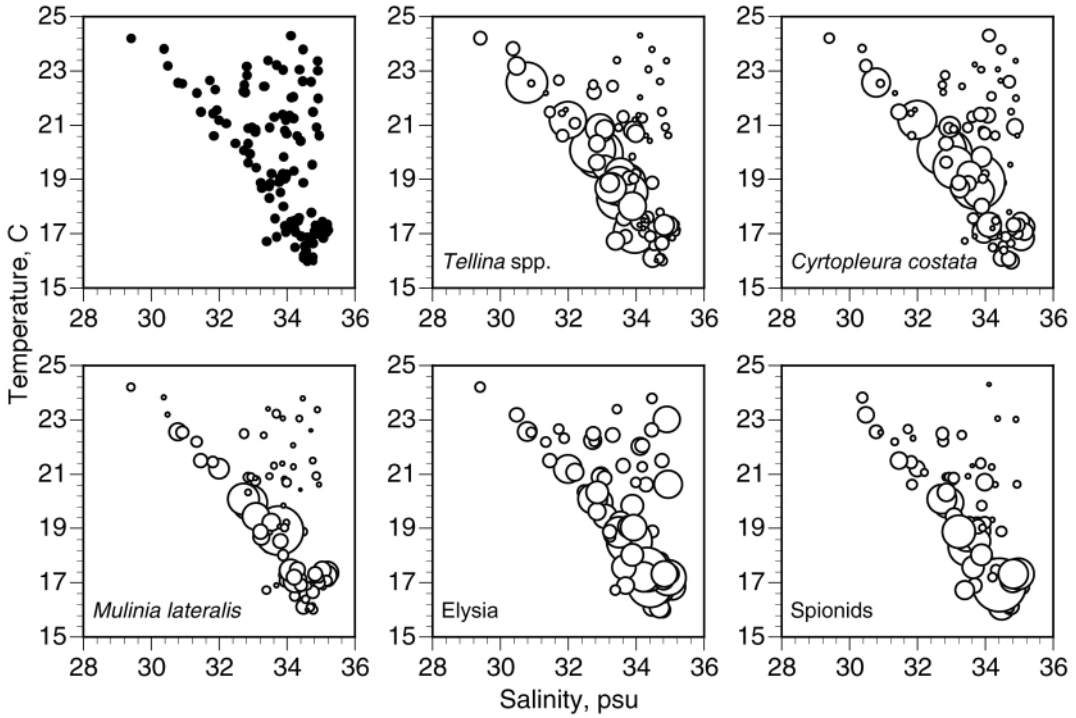

Fig. 12. Temperature/salinity diagram describing the relationship between temperature and salinity of the water in the study area and temperature/salinity bubble diagrams describing the relationship between the temperature and salinity of the water and the concentration of larvae in Cluster 2 in those waters. The size of the bubble is proportional to the concentration of larvae.

DISCUSSION

During August 12–13, wind-driven coastal upwelling was observed. Winds from the south-west had been blowing for 24 h prior to the beginning of the oceanographic sampling. The alongshore flow was generally to the north with an intensification of the alongshore flow nearshore. Cross-shelf flow above the pycnocline was generally offshore while below the pycnocline it tended to be onshore. Under the influence of the cross-shelf flow regime, the pycnocline was tilted upward towards the surface and, on most of the transects, it contacted the surface within 5 km of shore. In the most northern transect (3.0), there was a patch of surface water with salinity <30 p.s.u. indicative of Chesapeake Bay estuarine plume water. Patches of surface water with low salinity were also present on the transects to the south, but the salinity in these patches did not dip below 30 p.s.u. These conditions were typical for upwelling events during August when the water column was strongly stratified (Cudaback and Largier, 2001).

Per cent light transmission was high above the pycnocline (Figure 7). Lower light transmission values were observed below the pycnocline, with the lowest values observed within ~3 km of shore in the waters that were being advected towards the surface by upwelling. The generally lower light transmission adjacent to the bottom is probably the result of resuspension of fine particles. The lower light transmission values found in the upwelling waters may be because of the mechanical concentration of sinking particulates in a zone of rising water (Franks, 1992, 1997). These particulates were probably not predominantly phytoplankton because the chlorophyll concentrations in these waters were low. The lower light transmission may be the result of the accumulation of small aggregates and fine sediment with sinking rates closer to the vertical velocity of the upwelling. Modelling studies suggest that particulates with sinking rates similar to the rise rate of the water in a divergence will tend to accumulate in the divergence (Franks, 1992, 1997).

Over most of the study area, chlorophyll concentrations were low (Figure 8). High concentrations were only observed in distinct patches. Offshore patches were observed in three transects and a nearshore patch was found within 5 km of shore in each of the transects. The nearshore patches appear to have been associated with convergences and divergences in the flow field (Figure 6).

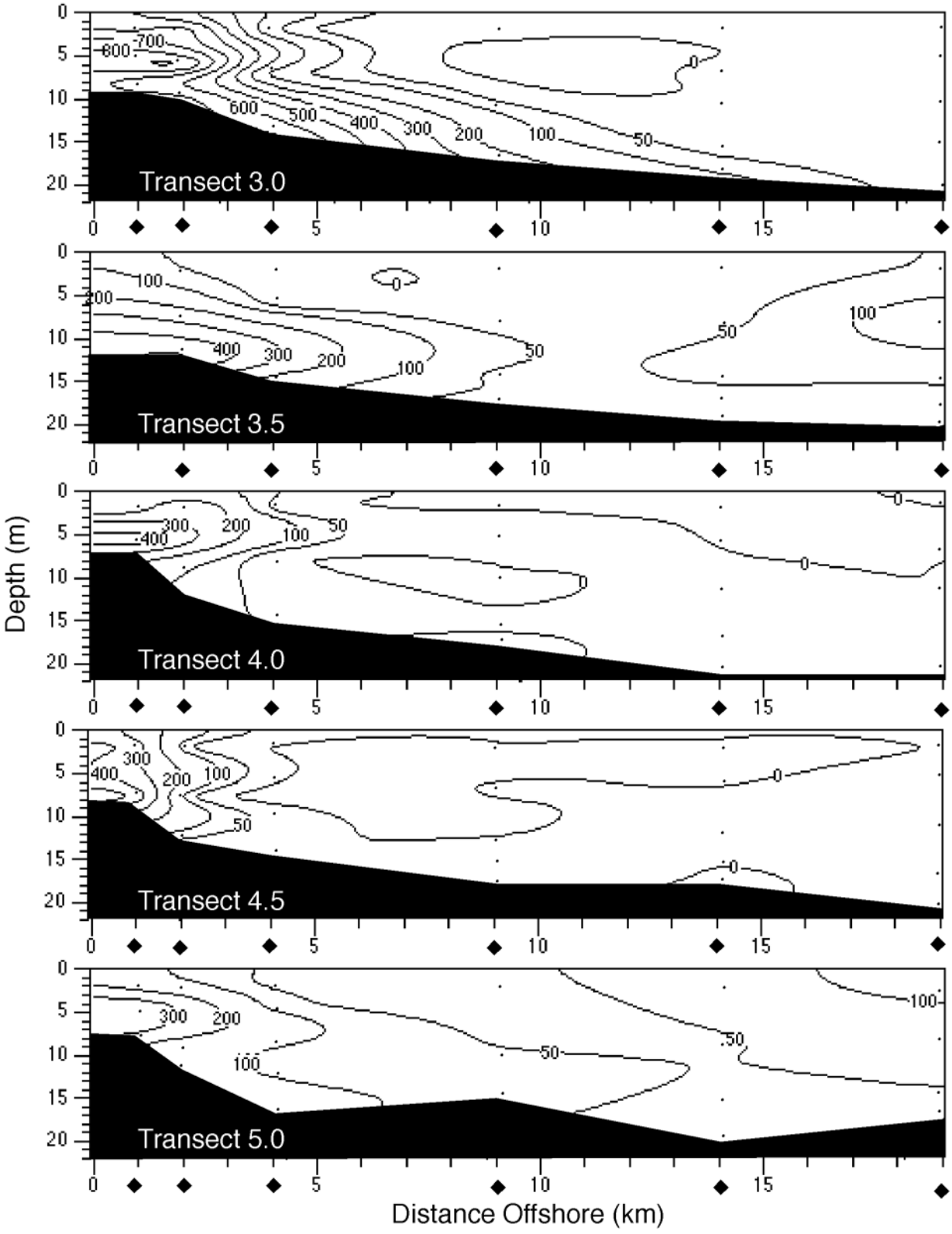

Fig. 13. Contour plots of *Tellina* sp. concentrations (no. m^{-3}), an example of a Cluster 2 or Cluster B larvae, along each of the transect lines. The black diamonds along the horizontal axes indicate station locations. Sample depths are indicated by the small dots.

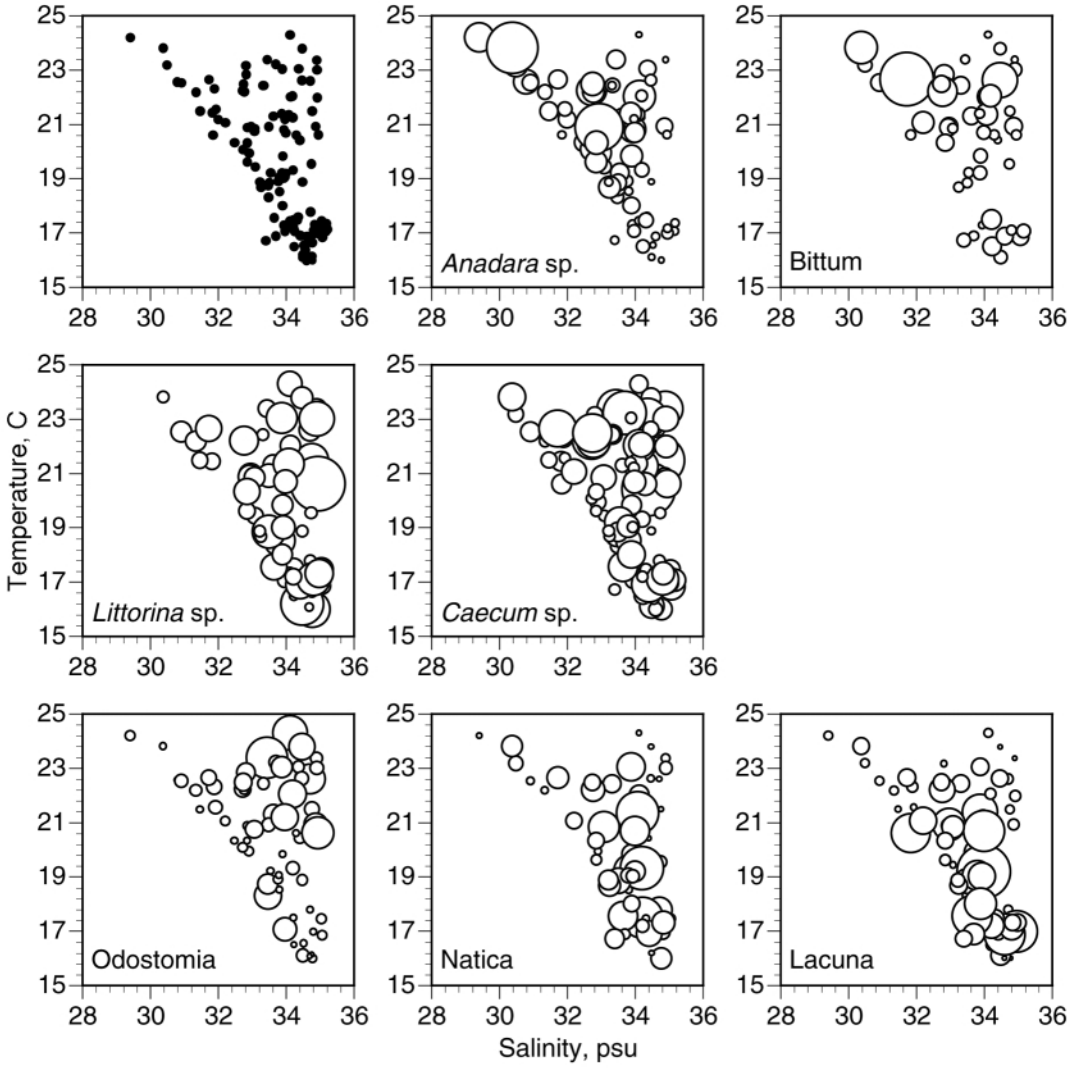

Fig. 14. Temperature/salinity diagram describing the relationship between temperature and salinity of the water in the study area and temperature/salinity bubble diagrams describing the relationship between the temperature and salinity of the water and the concentration of larvae in Cluster 3 in those waters. The size of the bubble is proportional to the concentration of larvae.

These results suggest that the patches of higher chlorophyll concentration may represent the physical accumulation of swimming phytoplankters within a convergent or divergent flow field (Franks, 1997; Lennert-Cody and Franks, 1999).

Along- or cross-shelf variations in the distribution of larvae could be the result of the effects of currents or either the input of new larvae from spawning or their removal by predation or settlement. The 100 μm mesh used in the plankton sampling retained few early stage larvae, and, thus, the input of spawned individuals did not confound the analysis. The sampling of the entire grid of stations took about a day, a short enough period that mortality because of predation should also not confound the analysis. Lastly, only a small proportion of the larvae were at a developmental stage competent to settle (L. Brink, unpublished data), suggesting that this source of variation on larval abundance is also probably of minimal influence.

We identified 22 different taxa (10 bivalve, nine gastropod and three polychaete). Twenty of these taxa were subjected to a cluster analysis from which three different clusters were identified. In an earlier paper (Shanks *et al.*, 2002), we presented the results of sampling carried out during a wind-driven downwelling event in the same location that took place ~2 weeks later in August. In this published study, larvae were much more abundant and we were able to identify 31 taxa which were divided into seven clusters. The decrease in the number of taxa present during the upwelling event was primarily the

result of the loss of three of the clusters that were present during the downwelling event. During the downwelling event, the plume of estuarine water from the Chesapeake Bay was very strong and extended along the coast through much of the study area. Six taxa formed the cluster of organisms associated with the plume [Cluster 3 in (Shanks *et al.*, 2002)]. Only one of these organisms (*Mercenaria mercenaria*) was present during the upwelling sampling. The five taxa found in the downwelling Clusters 5 or 6 were either absent or were not present in large enough numbers for analysis during the upwelling event. These taxa were not abundant or widely distributed in the samples from the downwelling event and were almost, or entirely, absent from the upwelling samples. In addition, two taxa that were present in sufficient numbers in the upwelling study (*Cratena* and *Hydrobia* in Cluster 1) were not present in the downwelling study samples. Despite the very large differences in the oceanographic conditions during the two sample grids, we found a fair amount of overlap in the composition of the clusters.

Upwelling Cluster 3 is the least interesting of the clusters defined in this present study. This cluster consisted of seven taxa; three taxa (*Lacuna*, *Natica* and *Odostomia*) comprised Cluster 4 in the downwelling study and the remaining taxa in the present cluster were members of a diversity of clusters in the downwelling study. The only relatively consistent pattern in the distribution of upwelling Cluster 3 organisms was that they all had a tendency to be found above the pycnocline either in the warmer offshore waters or nearshore in the remains of the estuarine plume. The individuals that composed Cluster 4 in the downwelling study were also found offshore above the pycnocline. Little more can be said about the distributions of the taxa in upwelling Cluster 3.

Excluding the taxa that were not present during the downwelling study (*Cratena* and *Hydrobia*), five of the remaining six taxa that composed the upwelling Cluster 1 were also members of the downwelling Cluster 1. *Mercenaria mercenaria* was a member of the downwelling Cluster 2; the cluster associated with the estuarine plume waters. During both the downwelling and upwelling events, the core taxa in these clusters had very similar distributions. In both cases they were found below the thermocline. During the downwelling event, the thermocline was bent downward by the flow regime and contacted the bottom some distance from shore. Organisms in the downwelling Cluster 1 tended to be found beyond 5 km from shore. During the upwelling event, the thermocline was bent upward by the flow and contacted the surface within 5 km of shore. In the upwelling data set, the taxa that comprised the upwelling Cluster 1 were still found below the thermocline, but they were found within 5 km of shore. The distributions of the organisms in these two clusters (upwelling Cluster 1 and downwelling Cluster 1) are consistent with the transport of the larvae relatively passively by the movement of the sub-thermocline waters; as the waters below the thermocline slosh back and forth with upwelling and downwelling events the organisms in these clusters appeared to have been transported back and forth across the shelf.

In the data from the upwelling event, there is some indication, however, that the organisms in Cluster 1 were not behaving entirely like passive particles. In the distributions of all the taxa that comprised upwelling Cluster 1 we found patches of high larval concentration within 5 km of shore within the waters that were being upwelled. The peak concentrations of larvae in the patches were, on average, five times the mean concentration of the larvae (range 3.4–10 times the mean concentration). The high concentrations suggest that larvae were accumulating in these nearshore patches. Typically the larvae in this cluster and downwelling Cluster 1 were found below the thermocline, the base of which was located below 10 m depth. The nearshore patches observed during the upwelling event tended to be found at depths <10 m. The high concentrations in the nearshore patches may be caused by the larvae in upwelling Cluster 1 swimming downward against the upwelling waters in an attempt to maintain a preferred depth below the pycnocline.

Downwelling Cluster 3 (Shanks *et al.*, 2002) and upwelling Cluster 2 (this study) share three taxa, *Tellina* sp., *C. costata* and *M. lateralis*. During the downwelling event, organisms in Cluster 3 tended to be widely distributed, but highly concentrated nearshore where the onshore surface flow encountered and downwelled under the Chesapeake Bay plume waters (Shanks *et al.*, 2002). In the upwelling event described here, Cluster 2 larvae were also widely distributed and highly concentrated nearshore. The highest concentrations were found just offshore where the pycnocline was being bent upward towards the surface by the upwelling process. Within the Cluster 2 organisms, the strongest and most consistent correlation was between the larval concentrations and the per cent light transmission; the highest larval concentrations were found in the waters with low light transmission and these waters were those that were being upwelled. Along each transect, larvae in upwelling Cluster 2 were found at high concentrations in patches nearshore. The peak concentration in these patches was, on average, 7.6 times the mean larval concentration (range 5.4–11 times the mean concentration).

In the data from the downwelling event, these larvae were concentrated in a convergence and downwelling zone. In the data from the upwelling event, these larvae were concentrated in a divergence and upwelling zone. The observed distributions may be the result of the same

simple behaviour: larvae attempt to maintain a desired depth and thereby become concentrated in either a convergence or divergence zone. In a convergence, the organism resists transport to a deeper depth by the flow field, while in a divergence it would swim downward against the rising current. In either case, the organisms will, over time, become concentrated in a patch (Franks, 1992, 1997). For this form of concentration to occur, the organism must be able to swim more rapidly than the rising or sinking current of the divergence or convergence. From Figure 6 one can estimate vertical speeds in our study by assuming negligible alongshore divergence $\delta v/\delta y$ and requiring that cross-shore divergence $\delta u/\delta x$ is balanced by vertical divergence $\delta w/\delta z$. Then integrating vertically from $w = 0$ at the surface or bottom boundary, one obtains vertical speeds $w = \int_0^d (\delta u/\delta x) \times \delta z$ at a distance d away from the boundary. Figure 6 indicates maximum possible values of 0.1 cm s^{-1} associated with 10-m-thick regions of maximum observed cross-shelf divergence $\delta u/\delta x = 10^{-5}$ s^{-1}. The swimming speeds of bivalves are in the range of 0.1 to 1 cm s^{-1}; swimming speeds fast enough to match or overcome the vertical flow field, thus allowing for concentration of the larvae (Chia *et al.*, 1984; Young, 1995). Within a system subjected to upwelling and downwelling and despite the large cross-shelf movements of water masses associated with shifts in the flow regime, a simple behaviour such as this—swimming to a preferred depth within a vertical flow field—has the potential to maintain larvae close to shore throughout their larval development.

The distribution of larvae may affect the pattern of settlement in time and space. There are five bivalve taxa shared by downwelling Cluster 1 (Shanks *et al.*, 2002) and upwelling Cluster 1 (this study). All have adult distributions that extend from the intertidal or shallow subtidal across much of the continental shelf. Given their observed distributions during downwelling (below the thermocline and mostly seaward of 5 km) and upwelling (below the thermocline with patches of high concentration landward of 5 km) we can hypothesize what the pattern of settlement may look like in these taxa. We hypothesize that, during the spawning season: (i) under a range of wind conditions, settlement at >5 km from shore will be fairly continuous; (ii) during downwelling events, larvae below the thermocline are transported offshore so that settlement will be mostly at distances >5 km from shore, and (iii) during upwelling events, larvae below the thermocline are swept shoreward so that settlement will occur <5 km from shore and settlement may be high beneath areas where larvae become concentrated by the convergence or divergence in the upwelling flow. Three bivalve taxa are shared by downwelling Cluster 3 (Shanks *et al.*, 2002) and upwelling Cluster 2 (this study). As adults, these taxa tend to be found in estuaries and sounds and in the shallow subtidal over the continental shelf. Under both downwelling- and upwelling-favourable winds, we found these larvae to be highly concentrated and continuously distributed within 5 km of shore. In this zone and during the spawning season, we predict settlement to be independent of the wind direction and fairly continuous in time and space. Seaward of 10 km from shore we predict that settlement will be light. We suggest that by their selection of a pelagic habitat and their behaviour within that habitat, these larvae may be going through their pelagic development in waters that bathe the benthic habitat into which they must ultimately settle.

It is a common assumption that the surface currents generated during wind-driven upwelling sweep larval invertebrates and fish offshore and that the reverse happens during downwelling events (Parrish *et al.*, 1981; Roughgarden *et al.*, 1988; Alexander and Roughgarden, 1996). This assumption should be particularly true for larvae that use cilia for propulsion; their slow swimming speed should put them at the mercy of wind-driven cross-shelf flow. The data presented here and in Shanks *et al.* (Shanks *et al.*, 2002) demonstrate clearly that this assumption is not necessarily true [see also (Peterson *et al.*, 1979)]. The distributions of some types of larvae indicate that they were swept back and forth across the shelf with the water mass changes generated by upwelling and downwelling; the distributions of these larvae appear to fit the assumption. The distributions of other species, however, indicate that they remained close to shore despite upwelling and downwelling currents; these larvae were not passively dispersed by the flow field. If bivalve larvae, slow-swimming larvae, can maintain nearshore distributions in the face of upwelling and downwelling currents and the complete exchange of the waters within the coastal boundary layer, then this level of control over cross-shelf transport is within the potential of essentially all types of larvae, both invertebrate and fish.

ACKNOWLEDGEMENTS

Field assistance was provided by K. Johnson, T. Rippietoe, M. Hearn, M. Amend, W. Waldorf and the Army Corps of Engineers Field Research Facility. Physical oceanographic data were provided by Dr S. Lentz and the Army Corps of Engineers Field Research Facility. This research was supported by the National Science Foundation, Coastal Ocean Processes Grants OCE-9123514, OCE-9633071, OCE-9221614 and OCE-9633013.

REFERENCES

Alexander, S. E. and Roughgarden, J. (1996) Larval transport and population dynamics of intertidal barnacles: a coupled benthic/oceanic model. *Ecol. Monogr.*, **66**, 259–275.

Bhaud, M. and Cazaux, C. (1982) Polychaete larvae from French coasts. *Oceanis*, **8**, 57–160.

Butman, C. A. (1994) CoOP: Coastal Ocean Processes Study: interdisciplinary approach, new technology to determine coupled biological, physical, geological processes affecting larval transport on the inner shelf. *Sea Technol.*, **1**, 44–49.

Chanley, P. and Andrews, J. D. (1971) Aids for identification of bivalve larvae of Virginia. *Malacologia*, **11**, 45–119.

Chia, F. S., Buckland-Nicks, J. and Young, C. M. (1984) Locomotion of marine invertebrate larvae: a review. *Can. J. Zool.*, **62**, 1205–1222.

Cudaback, C. N. and Largier, J. L. (2001) The cross-shelf structure of wind- and buoyancy-driven circulation over the North Carolina inner shelf. *Cont. Shelf Res.*, **21**, 1649–1668.

D'Sa, E., Lohrenz, S. E., Churchill, J. H., Apser, V., Largier, J. and Williams, A. J. (2001) Chloropigment distribution and transport on the inner shelf off Duck, North Carolina, USA. *J. Geophys. Res.*, **106**, 11581–11596.

Franks, P. J. S. (1992) Sink or swim: accumulation of biomass at fronts. *Mar. Ecol. Prog. Ser.*, **82**, 1–12.

Franks, P. J. S. (1997) Spatial patterns in dense algal blooms. *Limnol. Oceanogr.*, **42**, 1297–1305.

Gallager, S. M., Bidwell, J. P. and Kuzirian, A. M. (1989) Strontium is required in artificial seawater for embryonic shell formation in two species of bivalve molluscs. In Crick, R. (ed.), *Origin, Evolution, and Modern Aspects of Biomineralization in Plants and Animals*. Plenum Press, New York, pp. 349–365.

Garland, E. D., Zimmer, C. A. and Lentz, S. J. (2002) Larval distributions in inner-shelf waters: the roles of wind-driven cross-shelf currents and diel vertical migrations. *Limnol. Oceanogr.*, **47**, 803–817.

Kosro, P. M. and Huyer, A. (1986) CTD and velocity surveys of seaward jets off northern California, July 1981 and 1982. *J. Geophys. Res.*, **91**, 7680–7690.

Kosro, P. M., Barth, J. A. and Strub, P. T. (1997) The coastal jet: observations of surface currents over the Oregon continental shelf from HF radar. *Oceanography*, **10**, 53–56.

Lennert-Cody, C. E. and Franks, P. J. S. (1999) Plankton patchiness in high-frequency internal waves. *Mar. Ecol. Prog. Ser.*, **186**, 59–66.

Lentz, S., Carr, M. and Herbers, T. H. C. (2001) Barotropic tides on the North Carolina Shelf. *J. Phys. Oceanogr.*, **31**, 1843–1859.

Loosanoff, V. L., Davis, H. C. and Chanley, P. E. (1966) Dimensions and shapes of larvae of some marine bivalve mollusks. *Malacologia*, **4**, 351–435.

Mileikovsky, S. A. (1973) Speed of active movement of pelagic larvae of marine bottom invertebrates and their ability to regulate their vertical position. *Mar. Biol.*, **23**, 11–17.

Omori, M. and Ikeda, T. (1984) *Methods in Marine Zooplankton Ecology*. John Wiley & Sons, New York, 332 pp.

Parrish, R. H., Nelson, C. S. and Bakun, A. (1981) Transport mechanisms and reproductive success of fishes in the California Current. *Biol. Oceanogr.*, **1**, 175–203.

Peterson, W. T., Miller, C. B. and Hutchinson, A. (1979) Zonation and maintenance of copepod populations in the Oregon upwelling zone. *Deep Sea-Res.*, **26A**, 467–494.

Rees, C. B. (1950) The identification and classification of lamellibranch larvae. *Hull Bull. Mar. Ecol.*, **3**, 73–104.

Rennie, S. E. (1998) *Wind Interaction with Buoyant Plumes on the Inner Continental Shelf*. School of Marine Science The College of William and Mary, Gloucester Point, VA, 178 pp.

Rennie, S., Largier, J. and Lentz, S. (1999) Observations of a pulsed buoyancy current downstream of Chesapeake Bay. *J. Geophys. Res.*, **104**, 18227–18240.

Roughgarden, J., Gains, S. D. and Possingham, H. (1988) Recruitment dynamics in complex life cycles. *Science*, **241**, 1460–1466.

Rumrill, S. S. (1990) Natural mortality of marine invertebrate larvae. *Ophelia*, **21**, 163–198.

Shanks, A. L., Largier, J., Brink, L., Brubaker, J. and Hooff, R. (2002) Observations on the distribution of meroplankton during a downwelling event and associated intrusion of the Chesapeake Bay estuarine plume. *J. Plankton Res.*, **24**, 319–416.

StatSoft (1994) *Statistica for the Macintosh*. StatSoft, Tulsa.

Sullivan, C. M. (1948) Bivalve larvae of Malpeque Bay, P.E.I. *Fish. Res. Board Can. Bull.*, **LXXVII**, 1–36.

Thiriot-Quievreuz, C. (1980) Identification of some planktonic prosobranch larvae present off Beaufort, North Carolina. *Veliger*, **23**, 1–9.

Thorson, G. (1946) Reproduction and larval development of Danish marine bottom invertebrates, with special reference to the planktonic larvae in the sound (Oresund). *Medd. Dan. Fisk. Havunders. Ser. Plank.*, **4**, 1–523.

Venrick, E. L. (1978) How many cells to count? In Sournia, A. (ed.), *Phytoplankton Manual*. UNESCO, Paris, pp. 167–180.

Waldorf, B. W., Largier, J. L., Rennie, S., Austin, J. and Greengrove, C. (1995) *Coastal Ocean Process (CoOP) Pilot Projet Data Report: R/V Hatteras Shipboard Measurements; Underway, CTD and ADCP Data August 1994*. Scripps Institution of Oceanography, La Jolla, pp. 1–416.

Young, C. M. (1995) Behavior and locomotion during the dispersal phase of larval life. In McEdward, L. R. (ed.), *Ecology of Marine Invertebrate Larvae*. CRC Press, Boca Raton, pp. 249–278.

Received on December 10, 2002; accepted on February 10, 2003